Development 138, 1507-1519 (2011) doi:10.1242/dev.057802

Sox9 sustains chondrocyte survival and hypertrophy in part through Pik3ca-Akt pathways

Daisuke Ikegami[1,2], Haruhiko Akiyama[3], Akira Suzuki[4,5], Takashi Nakamura[3], Toru Nakano[6], Hideki Yoshikawa[2] and Noriyuki Tsumaki[1,2,7,*]

SUMMARY

During endochondral bone formation, Sox9 expression starts in mesenchymal progenitors, continues in the round and flat chondrocyte stages at high levels, and ceases just prior to the hypertrophic chondrocyte stage. Sox9 is important in mesenchymal progenitors for their differentiation into chondrocytes, but its functions post-differentiation have not been determined. To investigate Sox9 function in chondrocytes, we deleted mouse *Sox9* at two different steps after chondrocyte differentiation. Sox9 inactivation in round chondrocytes resulted in a loss of *Col2a1* expression and in apoptosis. Sox9 inactivation in flat chondrocytes caused immediate terminal maturation without hypertrophy and with excessive apoptosis. Inactivation of Sox9 in the last few cell layers resulted in the absence of *Col10a1* expression, suggesting that continued expression of Sox9 just prior to hypertrophy is necessary for chondrocyte hypertrophy. SOX9 knockdown also caused apoptosis of human chondrosarcoma SW1353 cells. These phenotypes were associated with reduced Akt phosphorylation. Forced phosphorylation of Akt by *Pten* inactivation partially restored *Col10a1* expression and cell survival in *Sox9*$^{floxdel/floxdel}$ mouse chondrocytes, suggesting that phosphorylated Akt mediates chondrocyte survival and hypertrophy induced by Sox9. When the molecular mechanism of Sox9-induced Akt phosphorylation was examined, we found that expression of the PI3K subunit Pik3ca (p110α) was decreased in *Sox9*$^{floxdel/floxdel}$ mouse chondrocytes. Sox9 binds to the promoter and enhances the transcriptional activities of *Pik3ca*. Thus, continued expression of Sox9 in differentiated chondrocytes is essential for subsequent hypertrophy and sustains chondrocyte-specific survival mechanisms by binding to the *Pik3ca* promoter, inducing Akt phosphorylation.

KEY WORDS: Sox9, Chondrocytes, Collagen, Conditional knockout, Transcriptional regulation, Mouse

INTRODUCTION

During development, the limb skeleton is created through endochondral bone formation. Mesenchymal cells initially undergo condensation, which is followed by the differentiation of prechondrogenic cells within these condensations into round chondrocytes, which proliferate and produce cartilage extracellular matrix to form cartilage primordia. Proliferating chondrocytes in the central region of the cartilage then exit the cell cycle and differentiate into prehypertrophic and, subsequently, hypertrophic chondrocytes. The proliferating chondrocytes closest to the prehypertrophic chondrocytes flatten out and form orderly columns of flat chondrocytes that are still proliferating. Finally, hypertrophic chondrocytes progress to terminal maturation to express matrix metalloproteinase 13 (Mmp13). Terminally mature chondrocytes undergo apoptosis. Blood vessels along with osteoblasts, osteoclasts and hematopoietic cells then invade and form primary ossification centers (Lefebvre and Smits, 2005). Cartilage at both ends of each skeletal component remains as articular cartilage and sustains joint movement.

Sox9 is a member of the SOX (Sry-related high mobility group box) family of transcription factors that share the high mobility group (HMG) DNA-binding motif with the mammalian testis-determining factor Sry. Heterozygous mutations in the human *SOX9* gene cause the skeletal malformation syndrome campomelic dysplasia (Foster et al., 1994; Wagner et al., 1994). Sox9 is expressed in progenitor cells in various organs (Akiyama et al., 2005), including chondroprogenitors, osteoprogenitors and preadipocytes (Wang and Sul, 2009), but is not expressed in most differentiated somatic cells such as osteoblasts and adipocytes (Wang and Sul, 2009), with the exception of chondrocytes. During endochondral bone formation, Sox9 expression starts in mesenchymal progenitor cells. Sox9 remains highly expressed in chondrocytes, and its expression ceases in prehypertrophic chondrocytes (Ng et al., 1997; Zhao et al., 1997). SOX9 expression continues in articular cartilage and decreases in osteoarthritic cartilage, a major cartilage disease caused by degeneration (Brew et al., 2010). That Sox9 plays a crucial role in mesenchymal progenitor cells has been established by analysis of *Sox9* knockout chimeras and conditional knockout mice. In mouse chimeras, *Sox9*$^{-/-}$ cells are excluded from cartilage primordia throughout embryonic development (Bi et al., 1999). Furthermore, mesenchymal condensation and subsequent cartilage formation are absent in the limbs of *Prx1-Cre; Sox9*$^{flox/flox}$ conditional knockout mice, in which the *Sox9* gene is inactivated in early mesenchymal limb bud cells before mesenchymal condensation occurs (Akiyama et al., 2002). In addition, the cartilage is very hypoplastic in *Col2a1-Cre; Sox9*$^{flox/flox}$ conditional knockout mice, in which Sox9

[1]Departments of Bone and Cartilage Biology, Osaka University Graduate School of Medicine, 2-2 Yamadaoka, Suita, Osaka 565-0871, Japan. [2]Department of Orthopaedic Surgery, Osaka University Graduate School of Medicine, 2-2 Yamadaoka, Suita, Osaka 565-0871, Japan. [3]Department of Orthopaedics, Graduate School of Medicine, Kyoto University, 54 Kawahara-cho, Shogoin, Sakyo-ku, Kyoto 606-8507, Japan. [4]Division of Cancer Genetics, Medical Institute of Bioregulation, Kyushu University, Fukuoka 812-8582, Japan. [5]Global Center of Excellence (COE) Program, Akita University Graduate School of Medicine, Akita 010-8543, Japan. [6]Department of Pathology, Medical School and Graduate School of Frontier Biosciences, Osaka University, Suita, Osaka 565-0871, Japan. [7]Japan Science and Technology Agency, CREST, Tokyo 102-0075, Japan.

*Author for correspondence (ntsumaki@dbcb.med.osaka-u.ac.jp)

Accepted 14 January 2011

expression is lost in condensed mesenchymal cells before differentiation into chondrocytes. In *Col2a1-Cre; Sox9$^{flox/flox}$* mice, *Sox9$^{floxdel/floxdel}$* cells remain as condensed mesenchymal cells and do not differentiate into chondrocytes (Akiyama et al., 2002).

The function of Sox9 expression post-differentiation into chondrocytes has not been determined. The functions of Sox9 in chondrocytes cannot be determined from previously reported chimeras or conditional knockout mice because they lack chondrocytes. Emerging evidence suggests that Sox9 inhibits chondrocyte hypertrophy; *Sox9$^{+/-}$* embryos show premature mineralization of cartilage and expanded hypertrophic zones (Bi et al., 2001). Mice that overexpress *Sox9* under the control of *Col2a1* regulatory elements exhibit delayed cartilage mineralization (Akiyama et al., 2004). In these genetically modified mice, however, the nature of the chondrocytes and matrix properties are altered before differentiation into chondrocytes owing to the manipulation of Sox9 expression from the stage of mesenchymal progenitor cells. A recent study has shown that misexpression of Sox9 in hypertrophic chondrocytes results in a lack of bone marrow, and that Sox9 is a major negative regulator of cartilage vascularization (Hattori et al., 2010).

We recently generated two types of transgenic mice in which Cre is expressed at different steps during chondrocyte differentiation (Iwai et al., 2008). In *11Enh-Cre* transgenic mice, Cre recombinase activities are controlled by the *Col11a2* promoter and enhancer and begin during the round chondrocyte stage. *11Enh-Cre* directs recombination at a later stage (both developmental and within the chondrocyte differentiation pathway) than *Col2a1-Cre*. Cre recombinase activities in *11Prom-Cre* transgenic mice are controlled by the *Col11a2* promoter alone and begin in the flat chondrocyte stage. In the present study, we examined the function of Sox9 in chondrocytes by generating *11Enh-Cre; Sox9$^{flox/flox}$* and *11Prom-Cre; Sox9$^{flox/flox}$* conditional knockout mice.

MATERIALS AND METHODS

Animals and genotyping

To generate *Sox9* conditional knockout mice, *11Enh-Cre* transgenic mice, *11Prom-Cre* transgenic mice (Iwai et al., 2008) and *Sox9$^{flox/flox}$* mice (Akiyama et al., 2002) were prepared and mated. To generate *Sox9; Pten* double conditional knockout mice, *Pten$^{flox/flox}$* mice (Suzuki et al., 2001) were prepared. For genotyping, genomic DNA was isolated from tail tips or embryonic skin and subjected to PCR analysis according to the methods previously described for the *Cre* transgene (Iwai et al., 2008), *Sox9* allele (Akiyama et al., 2002) and *Pten* allele (Suzuki et al., 2001).

Real-time RT-PCR

Total RNA was extracted using the RNeasy Mini Kit (Qiagen). Total RNAs were digested with DNase to eliminate any contaminating genomic DNA. PCR amplification was with SYBR Premix ExTaq (Takara) on a 7900HT real-time PCR system (Applied Biosystems). RNA expression levels were normalized to that of *Gapdh*. The primers used are listed in Table S1 in the supplementary material.

Staining of the skeleton

Embryos were dissected, fixed in 100% ethanol overnight, and then stained with Alcian Blue followed by Alizarin Red S solution according to standard protocols (Peters, 1977).

Histological analysis

Embryos were dissected under a stereomicroscope, fixed in 4% paraformaldehyde, processed and embedded in paraffin. For immunohistochemistry, sections were incubated with primary antibodies (Table 1). Immune complexes were detected using secondary antibodies conjugated to Alexa Fluor 488 (Table 1). RNA in situ hybridization was performed using ^{35}S-labeled antisense riboprobes as previously described (Pelton et al., 1990) or using a DIG RNA labeling kit (Boehringer Mannheim, Indianapolis, IN, USA) according to the manufacturer's instructions. In situ hybridization and immunohistochemistry were performed at least three times for each analysis.

BrdU staining

Pregnant mice were intraperitoneally injected with BrdU labeling reagent (10 μl/g body weight; Zymed Laboratories, South San Francisco, CA, USA). Two hours later, the mice were sacrificed and embryos were dissected and sectioned. Incorporated BrdU was detected using a BrdU staining kit (Zymed Laboratories) to distinguish actively proliferating cells. The average number of BrdU-positive cells among total cells (± s.d.) was calculated.

TUNEL assay

TUNEL assays were performed on semi-serial sections using the DeadEnd Fluorometric TUNEL System (Promega) according to the manufacturer's protocol.

Microscopy

Images were acquired on an inverted microscope (Eclipse Ti, Nikon) equipped with cameras (DS-Fi1, Nikon; C4742-80-12AG, Hamamatsu Photonics) and NIS Elements software (Nikon).

Table 1. Antibodies used in western blots and immunohistochemistry (IHC)

Antibody	Source (Cat. No.)	Dilution	
		Western	IHC
Anti-type I collagen	Abcam (ab34710)	–	1/1000
Anti-Sox9	Santa Cruz (sc-20095)	1/200	1/400
Anti-cleaved caspase 3	Cell Signaling (#9661)	–	1/100
Anti-Pten	Cell Signaling (#9559)	–	1/200
Anti-Pik3ca (p110α)	Cell Signaling (#4249)	1/1000	1/400
Anti-Pik3cb (p110β)	Cell Signaling (#3011)	1/1000	1/100
Anti-Pik3r1 and Pik3r2 (p85)	Cell Signaling (#4257)	1/1000	1/100
Anti-phospho-Akt	Cell Signaling (#4060)	1/1000	1/50
Anti-Akt	Cell Signaling (#4685)	1/1000	1/50
Anti-phospho-ATF2	Cell Signaling (#9221)	1/1000	1/100
Anti-ATF2	Cell Signaling (#9226)	1/1000	–
Anti-phospho-SAPK/JNK	Cell Signaling (#9251)	1/1000	1/100
Anti-phospho-p38 MAP kinase	Cell Signaling (#9211)	1/1000	1/100
Anti-p38 MAP kinase (MAPK14)	Cell Signaling (#9212)	1/1000	–
Anti-phospho-ERK1/2	Cell Signaling (#9101)	1/1000	–
Anti-ERK1/2 (MAPK3/1)	Cell Signaling (#4695)	1/1000	–
Anti-β-actin	Cell Signaling (#4967)	1/1000	–
Alexa Fluor 488 goat anti-rabbit	Invitrogen (A11008)	–	1/2000

Western blot analysis
Cell lysates were subjected to SDS-PAGE, electroblotted and immunostained with the antibodies listed in Table 1. Immunoblots were performed at least three times for each analysis.

Cell lines and cell culture
SW1353 (ATCC #HTB94), HeLa (Riken #RBC0007) and Saos2 (Riken #RCB0428) cells were cultured in Dulbecco's Modified Eagle's Medium (DMEM) supplemented with 10% fetal bovine serum (FBS) and 1% streptomycin/penicillin. ATDC5 cells were maintained at 20-80% confluency as described previously (Shukunami et al., 1996). For SOX9 overexpression experiments, SW1353 cells were transfected with the plasmid CMV promoter-SOX9 using Amaxa nucleofection technologies. Cells were harvested for real-time RT-PCR and immunoblot analysis 24 hours after transfection.

Knockdown of SOX9 via RNA interference
Amaxa nucleofection technology was used to transfect 1×10^6 SW1353, HeLa or Saos2 cells with 200 nM negative control siRNA (Stealth RNAi Negative Control Medium GC Duplex #2, 12935-112, Invitrogen) or SOX9-a, SOX9-b or SOX9-c siRNAs (Invitrogen Stealth RNAi; siRNA target sequences are listed in Table S2 in the supplementary material).

Six hours after transfection, cell lysates were collected for immunoblot analysis. For morphological evaluation, 1×10^6 cells were seeded into 6-well plates and 6 hours after transfection cells were stained with Hoechst 33342 (Dojindo Laboratories, Japan). Caspase 3/7 activities were measured 6 hours after transfection using the Caspase-Glo3/7 Assay Kit (Promega) according to the manufacturer's instructions. Six hours after transfection, the level of apoptosis was determined using the Cell Death Detection ELISA^{PLUS} Kit (Roche Applied Science).

Luciferase reporter assay
Various lengths of human *PIK3CA* promoter sequence (Hui et al., 2008) were prepared. Mutations were introduced using the GeneTailor Site-Directed Mutagenesis System (Invitrogen). Fragments were inserted into the pGL3-basic vector (Promega). Undifferentiated ATDC5 cells and SW1353 cells were co-transfected with 20 ng reporter construct, 10 ng phRL-TK (Promega) and a total of 200 ng SOX9 expression vector and mock vector using FuGENE (Roche). Cell lysates were collected 48 hours after transfection. Photinus luciferase activity levels were normalized to those of Renilla luciferase (phRL-TK).

Chromatin immunoprecipitation (ChIP) assay
A ChIP assay kit (Upstate #17-295) was used according to the manufacturer's protocol. The purified DNA was used as a template in PCR assays. The primers are listed in Table S3 in the supplementary material.

Statistical analyses
Data are shown as averages with standard deviations. Student's *t*-test was used to compare data. $P<0.05$ was considered statistically significant.

RESULTS

Generation of *11Enh-Cre; Sox9$^{flox/flox}$* conditional knockout mice

We initially intercrossed *11Enh-Cre* mice (Iwai et al., 2008) with *Sox9$^{flox/flox}$* mice (Akiyama et al., 2002). *Sox9$^{flox/+}$* heterozygotes that harbor *11Enh-Cre* were recovered with the expected Mendelian frequency (see Fig. S1A in the supplementary material); these mice were fertile and developed dwarfism (see Fig. S1B in the supplementary material). Eighty-five percent of *11Enh-Cre; Sox9$^{flox/+}$* mice were viable beyond 6 months of age (see Fig. S1C in the supplementary material), suggesting that these mice have a much milder phenotype than *Col2a1-Cre; Sox9$^{flox/+}$* mice, which have a 95% death rate by 10 days of age (Akiyama et al., 2002).

We then intercrossed *11Enh-Cre; Sox9$^{flox/+}$* mice with *Sox9$^{flox/flox}$* mice (see Fig. S1D in the supplementary material). The cartilage and bone of *11Enh-Cre; Sox9$^{flox/flox}$* embryos at 16.5 days post-coitum (dpc) were very hypoplastic, whereas the calvarium, which undergoes membranous ossification and is formed without cartilage templates, appeared to be well formed (see Fig. S1E-G in the supplementary material).

11Enh-Cre; Sox9$^{flox/flox}$ mice start to lose Sox9 expression in round chondrocytes, resulting in apoptosis

Histological analysis showed that *11Enh-Cre; Sox9$^{flox/flox}$* conditional knockout embryos exhibited normal mesenchymal condensation with normal Sox9 expression patterns in paws at 12.5 dpc (Fig. 1A). At 12.5 dpc, cells in the central region of mesenchymal condensation at the humerus differentiated into round chondrocytes, as indicated by round or polygonal cell morphologies and slight staining of the surrounding matrix with Safranin O in control *Sox9$^{flox/+}$* embryos (Fig. 1B, left column). Round chondrocytes in the central region of condensation in *11Enh-Cre; Sox9$^{flox/flox}$* humerus showed decreased staining of the matrix with Safranin O and lost Sox9 expression (Fig. 1B, right column). These results suggest that *11Enh-Cre* initiated the direct recombination of floxed *Sox9* genes in round chondrocytes. At 13.5 dpc, the primordial cartilage of control *Sox9$^{flox/+}$* mouse humerus was formed, as indicated by Safranin O staining (Fig. 1C). Immunohistochemistry with anti-Sox9 antibodies showed that proliferative chondrocytes in cartilage expressed Sox9. By contrast, primordial cartilage in *11Enh-Cre; Sox9$^{flox/flox}$* humerus was disorganized at 13.5 dpc, with weak Safranin O staining intensities, and the chondrocytes in the central region of cartilage had lost Sox9 expression. Cells in the periphery of the primordial cartilage still expressed Sox9. *Col2a1* expression was lost in accordance with the loss of Sox9. This in vivo result supports the notion that Sox9 is needed for the maintenance of *Col2a1* transcription in chondrocytes. Hypertrophic chondrocytes were absent and *Col10a1* expression was lost. At 14.5 dpc, *11Enh-Cre; Sox9$^{flox/flox}$* humerus showed only a small amount of cartilage, which was disorganized and lacked hypertrophic chondrocytes (Fig. 1D). *Ihh* expression was almost completely lost and expression of *Col10a1* and *Mmp13* was lost. Runx2 expression was maintained in bone collars. These results suggest that *Sox9* deletion in round chondrocytes abolishes the subsequent differentiation of chondrocytes.

Together with an existing report that the loss of Sox9 is associated with apoptosis in neural crest cells (Cheung et al., 2005), the presence of just a small amount of disorganized cartilage, despite the initial mesenchymal condensation, raised the possibility that chondrocytes underwent apoptosis. We found that cells were TUNEL negative and did not show immunoreactivity for cleaved caspase 3 in either *11Enh-Cre; Sox9$^{flox/flox}$* or *Sox9$^{flox/+}$* humerus at 12.5 dpc (see Fig. S2A in the supplementary material). Cells in the epiphyseal region within the disorganized cartilage in *11Enh-Cre; Sox9$^{flox/flox}$* humerus showed TUNEL staining and immunoreactivity for cleaved caspase 3, whereas chondrocytes in the control *Sox9$^{flox/+}$* humerus did not at 13.5 dpc (Fig. 1E). As for positive controls, TUNEL-positive cells were detected in the interdigital regions of paws of both control *Sox9$^{flox/+}$* and *11Enh-Cre; Sox9$^{flox/flox}$* embryos at 13.5 dpc (see Fig. S2B in the supplementary material). These results suggest that epiphyseal chondrocytes undergo apoptosis ~1 day after deletion of *Sox9* in round chondrocytes.

Disorganized primary ossification centers were formed in *11Enh-Cre; Sox9$^{flox/flox}$* humerus at 15.5 dpc (see Fig. S2C in the supplementary material). *Col2a1* expression was almost completely

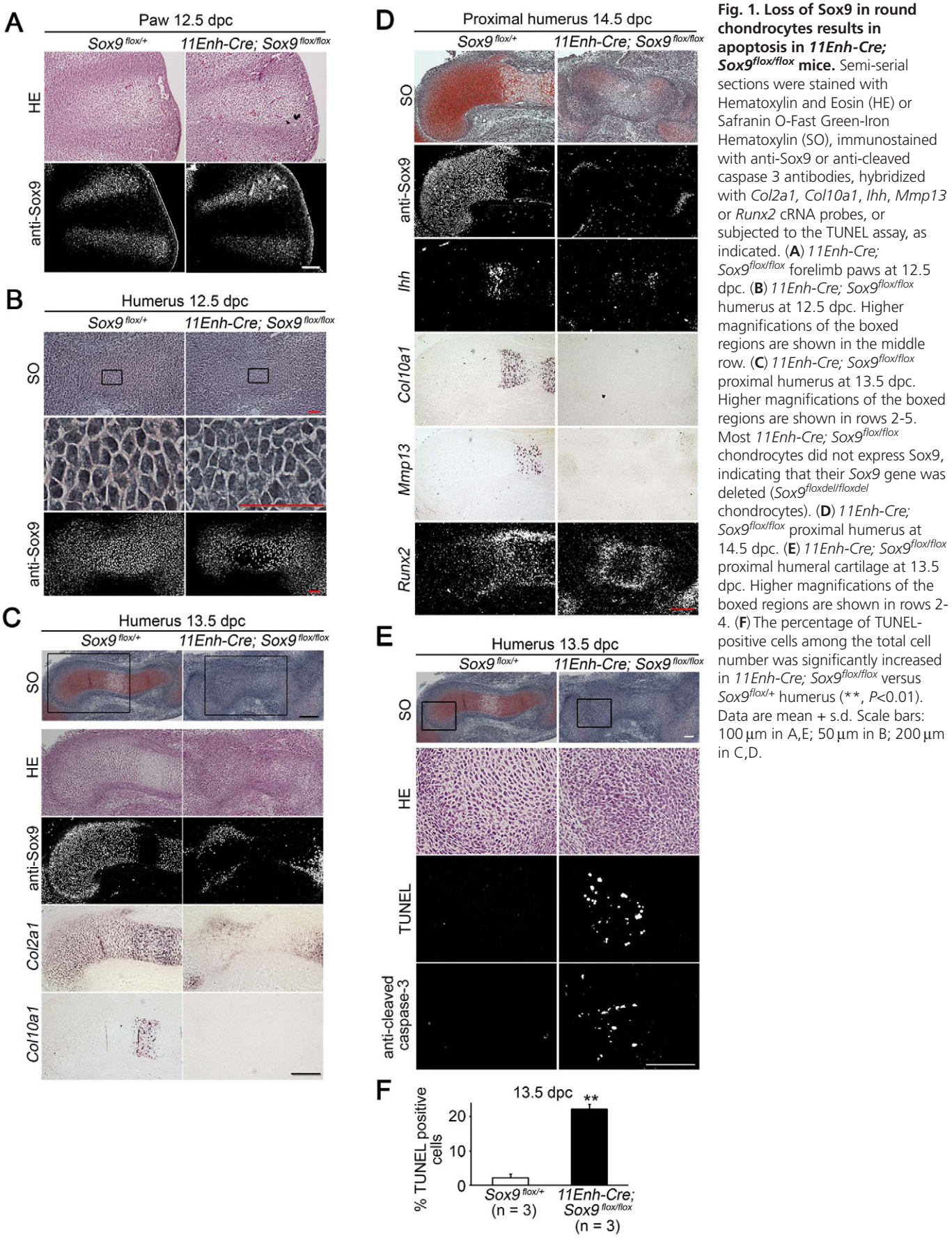

Fig. 1. Loss of Sox9 in round chondrocytes results in apoptosis in *11Enh-Cre; Sox9$^{flox/flox}$* mice. Semi-serial sections were stained with Hematoxylin and Eosin (HE) or Safranin O-Fast Green-Iron Hematoxylin (SO), immunostained with anti-Sox9 or anti-cleaved caspase 3 antibodies, hybridized with *Col2a1*, *Col10a1*, *Ihh*, *Mmp13* or *Runx2* cRNA probes, or subjected to the TUNEL assay, as indicated. (**A**) *11Enh-Cre; Sox9$^{flox/flox}$* forelimb paws at 12.5 dpc. (**B**) *11Enh-Cre; Sox9$^{flox/flox}$* humerus at 12.5 dpc. Higher magnifications of the boxed regions are shown in the middle row. (**C**) *11Enh-Cre; Sox9$^{flox/flox}$* proximal humerus at 13.5 dpc. Higher magnifications of the boxed regions are shown in rows 2-5. Most *11Enh-Cre; Sox9$^{flox/flox}$* chondrocytes did not express Sox9, indicating that their *Sox9* gene was deleted (*Sox9$^{floxdel/floxdel}$* chondrocytes). (**D**) *11Enh-Cre; Sox9$^{flox/flox}$* proximal humerus at 14.5 dpc. (**E**) *11Enh-Cre; Sox9$^{flox/flox}$* proximal humeral cartilage at 13.5 dpc. Higher magnifications of the boxed regions are shown in rows 2-4. (**F**) The percentage of TUNEL-positive cells among the total cell number was significantly increased in *11Enh-Cre; Sox9$^{flox/flox}$* versus *Sox9$^{flox/+}$* humerus (**, $P<0.01$). Data are mean + s.d. Scale bars: 100 μm in A,E; 50 μm in B; 200 μm in C,D.

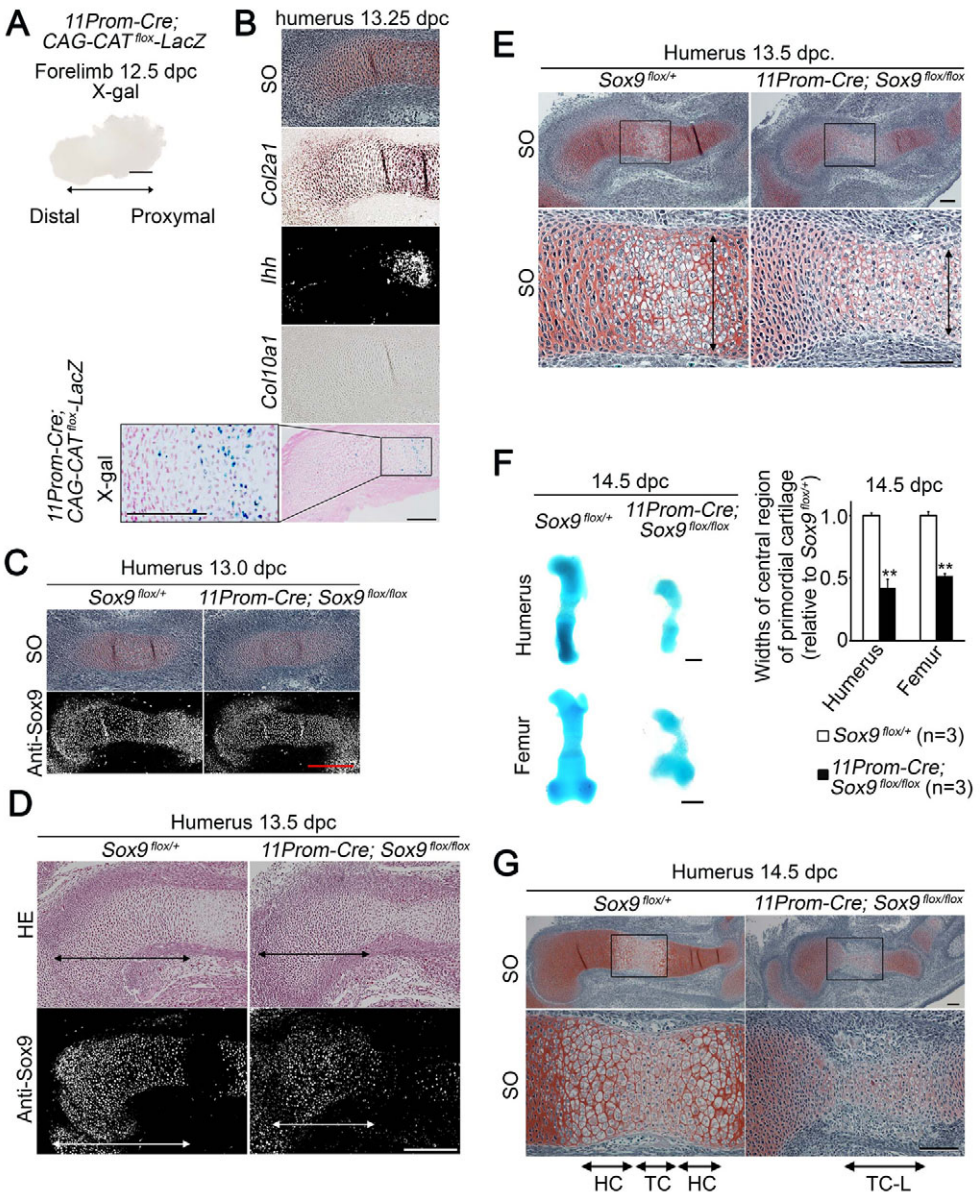

Fig. 2. Premature shutdown of Sox9 expression in flat chondrocytes results in a loss of hypertrophic chondrocytes in *11Prom-Cre; Sox9$^{flox/flox}$* mice. Semi-serial sections were stained with HE, SO or for *lacZ* expression (X-gal), immunostained with anti-Sox9, or hybridized with *Col2a1, Col10a1* or *Ihh* cRNA probes as indicated. (**A**,**B**) Cre-mediated recombination patterns of *11Prom-Cre* analyzed by mating with *CAG promoter-flox-CAT-flox-lacZ* transgenic tester mice. *lacZ* activity was detected in several layers of chondrocytes in the humerus at 13.25 dpc, which is when prehypertrophy starts at the center of the primordial cartilage as indicated by *Ihh* expression. (**C**) *11Prom-Cre; Sox9$^{flox/flox}$* versus *Sox9$^{flox/+}$* humerus at 13.0 dpc. (**D**) *11Prom-Cre; Sox9$^{flox/flox}$* humerus at 13.5 dpc shows a shorter zone (arrows) of proliferative chondrocytes that expressed Sox9 than the *Sox9$^{flox/+}$* control. (**E**) The width of the central region of primordial cartilage in *11Prom-Cre; Sox9$^{flox/flox}$* humerus at 13.5 dpc was decreased. Higher magnifications of the boxed regions are shown beneath. (**F**) Cartilaginous skeletons were stained with Alcian Blue. Data are mean ± s.d.; **, $P<0.01$. (**G**) The central region of the control *Sox9$^{flox/+}$* humerus consisted of a terminally mature chondrocyte zone (TC) flanked by hypertrophic chondrocyte zones (HC). The central region of the *11Prom-Cre; Sox9$^{flox/flox}$* humerus lacked hypertrophic chondrocyte zones and contained cells that resembled terminally mature chondrocytes (TC-L). Higher magnifications of the boxed regions are shown beneath. Scale bars: 200 μm in A-D,F; 100 μm in E,G.

lost and expression of *Ihh* and *Col10a1* was lost. Expression of *Mmp13* was lost in chondrocytes but maintained in the primary ossification center. Bone in the primary ossification center could have been formed by endochondral ossification through abnormal chondrocytes that survived after *Sox9* deletion or by membranous ossification from the bone collar.

Generation of *11Prom-Cre; Sox9$^{flox/flox}$* conditional knockout mice

We intercrossed *11Prom-Cre* mice (Iwai et al., 2008) with *Sox9$^{flox/flox}$* mice (Akiyama et al., 2002) to examine Sox9 function in chondrocytes at a later stage of differentiation. *11Prom-Cre; Sox9$^{flox/+}$* mice were recovered with the expected Mendelian frequency (see Fig. S3A in the supplementary material), developed normally and showed similar crown-rump lengths as control *Sox9$^{flox/+}$* mice 3 weeks after birth (see Fig. S3B in the supplementary material). *11Prom-Cre; Sox9$^{flox/flox}$* embryos were recovered with the expected Mendelian frequency from 12.5-16.5 dpc (see Fig. S3C in the supplementary material). The skeleton was very hypoplastic, whereas the calvarium appeared to be well formed (see Fig. S3D-G in the supplementary material). The cartilage of the limb buds and vertebral bodies was very hypoplastic.

11Prom-Cre; Sox9$^{flox/flox}$ mice start to lose Sox9 expression in flat chondrocytes closest to prehypertrophic chondrocytes

Cre-mediated recombination patterns of *11Prom-Cre* were analyzed by mating *11Prom-Cre* transgenic mice with *CAG promoter-flox-CAT-flox-lacZ* transgenic tester mice (Sakai and Miyazaki, 1997). No recombination was detected in limbs at 12.5 dpc (Fig. 2A). *lacZ* activity was detected in several layers of chondrocytes in the humerus at 13.25 dpc, which is when prehypertrophy starts at the center of the primordial cartilage. In situ hybridization analysis of sections from different samples at the same stage of 13.25 dpc showed that recombination started to occur in *Ihh*-expressing cells

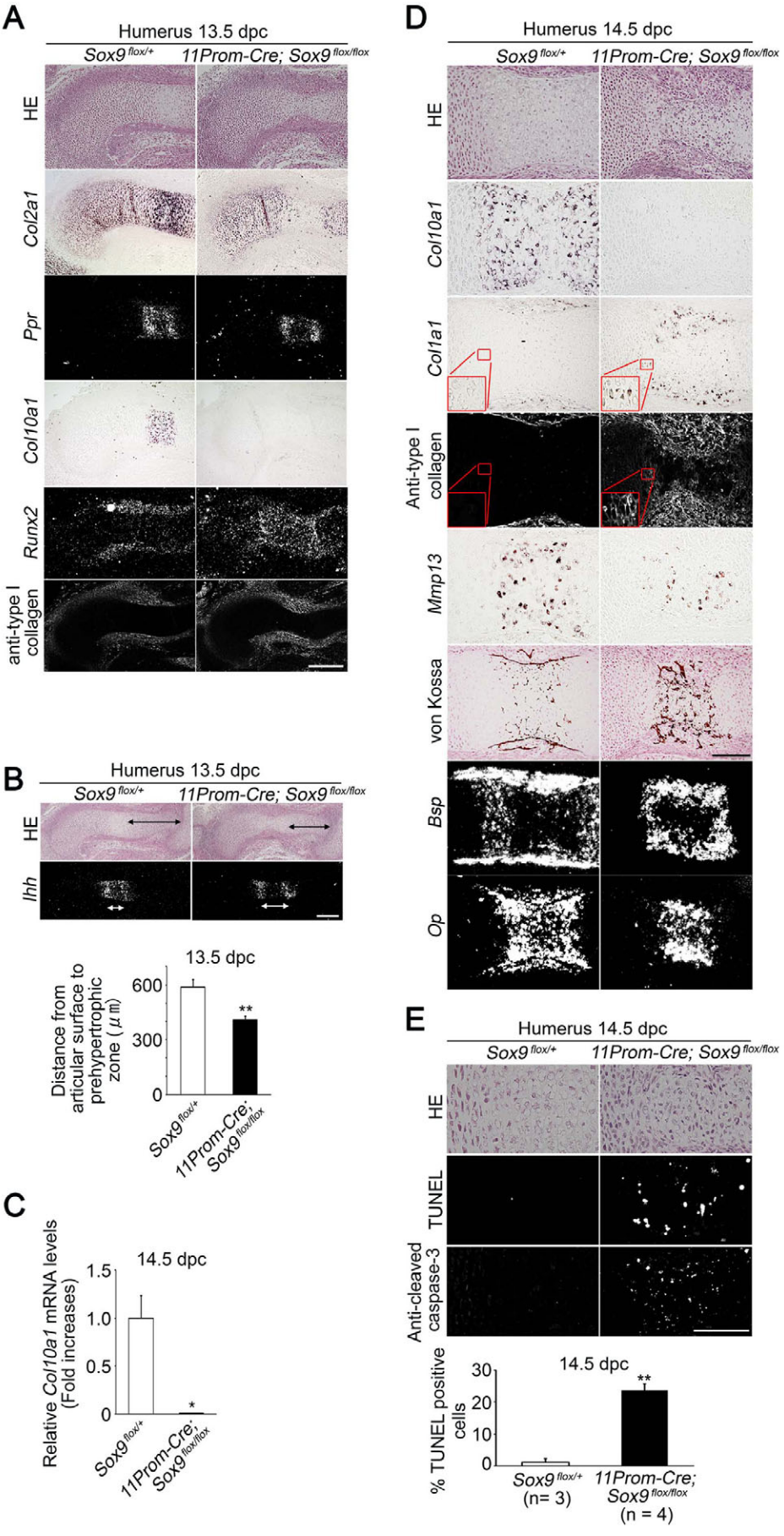

Fig. 3. Shift of prehypertrophy towards articular ends, absence of hypertrophy, and enhanced apoptosis in chondrocytes of *11Prom-Cre; Sox9$^{flox/flox}$* mice. Semi-serial sections were stained with HE or von Kossa, immunostained with anti-cleaved caspase 3 or type I collagen antibodies, hybridized with the indicated cRNA probes, or subjected to the TUNEL assay, as labeled. (**A**) Proximal humerus at 13.5 dpc. (**B**) Humerus at 13.5 dpc. *n*=3. (**C**) Real-time RT-PCR analysis of *Col10a1* expression in the humerus. The control *Sox9$^{flox/+}$* expression level was set at 1. *n*=3. (**D**) Semi-serial sections of the central region of humeral cartilage at 14.5 dpc. (**E**) Semi-serial sections of the central region of humeral cartilage at 14.5 dpc. The percentage of TUNEL-positive cells among the total cell number was significantly increased in *11Prom-Cre; Sox9$^{flox/flox}$* versus *Sox9$^{flox/+}$* humerus. Data (B,C,E) are mean + s.d. *, $P<0.05$; **, $P<0.01$. Scale bars: 200 μm in A,B; 100 μm in D,E.

(Fig. 2B). At later stages, cells closest to the prehypertrophic chondrocytes subsequently flattened out and formed orderly columns of flat chondrocytes in which *11Prom-Cre* directs recombination (Iwai et al., 2008).

Histological analysis showed that *11Prom-Cre; Sox9$^{flox/flox}$* conditional knockout mice form primordial cartilage normally in the humerus and a normal Sox9 expression pattern is present at 13.0 dpc (Fig. 2C). At 13.5 dpc, the humerus of *Sox9$^{flox/+}$* control mice showed prehypertrophy and hypertrophy of chondrocytes in the central region of cartilage primordia. Proliferative chondrocyte-specific expression of Sox9 abruptly stopped when chondrocytes entered into the prehypertrophic stage in control mice. The length (proximodistal direction) of the zone of proliferative chondrocytes expressing Sox9 in *11Prom-Cre; Sox9$^{flox/flox}$* humerus was 25% shorter than that in *Sox9$^{flox/+}$* control humerus (Fig. 2D, arrows). These results suggest that Sox9 expression was lost in several layers of flat chondrocytes closest to the prehypertrophic chondrocytes in *11Prom-Cre; Sox9$^{flox/flox}$* humerus.

The width (transverse direction) of the central region of the primordial cartilage was decreased in *11Prom-Cre; Sox9$^{flox/flox}$* mouse humerus at 13.5 dpc, and the humerus had a dumb-bell-shaped appearance (Fig. 2D,E). The dumb-bell shape was confirmed by Alcian Blue staining of the skeleton at 14.5 dpc (Fig. 2F). The zone of hypertrophic chondrocytes and the zone of terminally mature chondrocytes were formed in the center of *Sox9$^{flox/+}$* control humerus at 14.5 dpc. By contrast, the hypertrophic chondrocytes were absent and cells that resembled terminally mature chondrocytes were present in the center of the *11Prom-Cre; Sox9$^{flox/flox}$* humerus (Fig. 2G).

11Prom-Cre; Sox9$^{flox/flox}$ flat chondrocytes undergo prehypertrophy, skip hypertrophy and undergo vigorous apoptosis

We analyzed the expression of marker genes at 13.5 dpc. The expression pattern of *Col2a1* mRNAs (Fig. 3A) corresponded almost exactly to that of Sox9 proteins in *11Prom-Cre; Sox9$^{flox/flox}$* humerus (Fig. 2D). *Ppr* (receptor for parathyroid hormone and parathyroid hormone-related peptides; *Pth1r* – Mouse Genome Informatics) mRNAs were detected in *11Prom-Cre; Sox9$^{flox/flox}$* humerus (Fig. 3A). Hypertrophic chondrocyte marker type X collagen (*Col10a1*) mRNA was detected in the center of *Sox9$^{flox/+}$* cartilage, but not in *11Prom-Cre; Sox9$^{flox/flox}$* cartilage. *Runx2* mRNA was strongly detected in bone collars of primordial cartilage and weakly detected in chondrocytes in *Sox9$^{flox/+}$* humerus. *Runx2* expression in chondrocytes appeared to increase in *11Prom-Cre; Sox9$^{flox/flox}$* humerus. The bone collar was thickened and type I collagen expression in the bone collar increased in *11Prom-Cre; Sox9$^{flox/flox}$* humerus. The distances (Fig. 3B, black arrows) between the distal articular surface and prehypertrophic zone indicated by *Ihh* expression were reduced in *11Prom-Cre; Sox9$^{flox/flox}$* humerus (Fig. 3B, bar chart). The distance (Fig. 3B, white arrows) between the two zones of *Ihh*-positive cells was increased in *11Prom-Cre; Sox9$^{flox/flox}$* humerus. These results, together with the Sox9 expression patterns (Fig. 2D), suggest that the premature shutdown of Sox9 in several cell layers of flat chondrocytes caused a shift of *Ihh* expression toward the articular surfaces of primordial cartilage and an absence of *Col10a1* expression.

The abnormalities found in *11Prom-Cre; Sox9$^{flox/flox}$* cartilage at 13.5 dpc were enhanced at 14.5 dpc. In control *Sox9$^{flox/+}$* humerus, flat chondrocytes, which had emerged next to prehypertrophic chondrocytes at 13.5 dpc, dramatically increased in number in the metaphyseal zones at 14.5 dpc. The number of chondrocytes in the metaphyseal zone of *11Prom-Cre; Sox9$^{flox/flox}$* humerus was decreased as compared with the control *Sox9$^{flox/+}$* humerus (see Fig. S4A in the supplementary material, top row, outlined region). Sox9 expression was only detected in epiphyseal round chondrocytes in *11Prom-Cre; Sox9$^{flox/flox}$* humerus, whereas Sox9 was expressed both in epiphyseal round and metaphyseal flat chondrocytes in the control *Sox9$^{flox/+}$* humerus. These results indicate that metaphyseal proliferative chondrocytes in *11Prom-Cre; Sox9$^{flox/flox}$* humerus are *Sox9$^{floxdel/floxdel}$* proliferative chondrocytes (see Fig. S4A in the supplementary material, right panels, outlined region). The expression patterns of *Col2a1* and *Col11a2* corresponded to those of Sox9 proteins. *Ppr* was expressed, but *Col10a1* expression was lost in *11Prom-Cre; Sox9$^{flox/flox}$* cartilage. Real-time RT-PCR analysis of RNA from the humerus confirmed a significant decrease in *Col10a1* expression (Fig. 3C).

Col1a1 mRNAs and proteins were ectopically expressed in the chondrocytes in the central region of *11Prom-Cre; Sox9$^{flox/flox}$* humeral cartilage at 14.5 dpc (Fig. 3D). Together with the cell morphology (Fig. 2G, TC-L), the expression of *Mmp13*, bone sialoprotein (*Bsp*; *Ibsp* – Mouse Genome Informatics) mRNA and osteopontin (*Op*; *Spp1* – Mouse Genome Informatics) mRNA (Fig. 3D) strongly suggest that these cells are terminally mature chondrocytes. The absence of *Col10a1*-expressing cells and the reduced number of *Mmp13*-, *Bsp*- and *Op*-expressing cells suggest that *Sox9* deletion in flat chondrocytes severely inhibits subsequent hypertrophy and moderately inhibits terminal maturation. Mineralization of chondrocytes in the central region of the cartilage was increased. Cells were TUNEL negative and did not show immunoreactivity for cleaved caspase 3 in *11Prom-Cre; Sox9$^{flox/flox}$* humerus at 13.5 dpc (see Fig. S4B in the supplementary material). Significant apoptosis associated with the expression of cleaved caspase 3 was detected in the zone of terminally mature chondrocytes (Fig. 3E) at 14.5 dpc. These results suggest that *Sox9* deletion started in flat chondrocytes at 13.5 dpc and that chondrocytes lacking Sox9 undergo abnormal differentiation (severe inhibition of hypertrophy and moderate inhibition of terminal differentiation) into terminally mature chondrocytes, where excess apoptosis is detected at 14.5 dpc.

BrdU labeling analysis (see Fig. S4C in the supplementary material) revealed increased proliferation of perichondrial bone collar cells in *11Prom-Cre; Sox9$^{flox/flox}$* humeral cartilage at 13.5 dpc; this increased proliferation was responsible for the thick bone collar (Fig. 2D). Proliferation rates in metaphyseal zone chondrocytes in *11Prom-Cre; Sox9$^{flox/flox}$* humeral cartilage decreased at 14.5 dpc; this decreased proliferation caused a corresponding decrease in the length of the zone of metaphyseal chondrocytes (see Fig. S4A in the supplementary material).

Our results indicate that flat chondrocytes lacking Sox9 expression are characterized by the cessation of *Col2a1* expression, decreased proliferation rates, a reduced cell population, a shift of prehypertrophy towards the articular end, and a lack of hypertrophy; these chondrocytes immediately enter into terminal maturation associated with ectopic type I collagen expression in the cartilage matrix, undergo increased apoptosis and stimulate the proliferation of bone collar cells. Thus, Sox9 is needed for subsequent chondrocyte hypertrophy. This phenotype is similar to those of *Sox5$^{-/-}$; Sox6$^{-/-}$* (Smits et al., 2001), *Sox5$^{+/-}$;Sox6$^{-/-}$* and *Sox5$^{-/-}$;Sox6$^{+/-}$* mice (Smits et al., 2004). *Sox5$^{-/-}$; Sox6$^{-/-}$* mice lack columnar chondrocytes and *Col10a1* expression, but they do have prehypertrophic

chondrocytes and express *Mmp13*. Because Sox5 and Sox6 facilitate the organization of transcription complexes (Lefebvre and Smits, 2005), the phenotypic similarities between *11Prom-Cre; Sox9*$^{flox/flox}$ mice and *Sox5*$^{-/-}$*; Sox6*$^{-/-}$ mice suggest that the *Sox9* conditional knockout phenotype is due to dysfunction of transcription complexes containing Sox5, Sox6 and Sox9. The observation that chondrocytes lacking Sox9 enter into terminal maturation without hypertrophy is consistent with findings that Sox9 misexpression in hypertrophic chondrocytes inhibits their terminal maturation (Hattori et al., 2010).

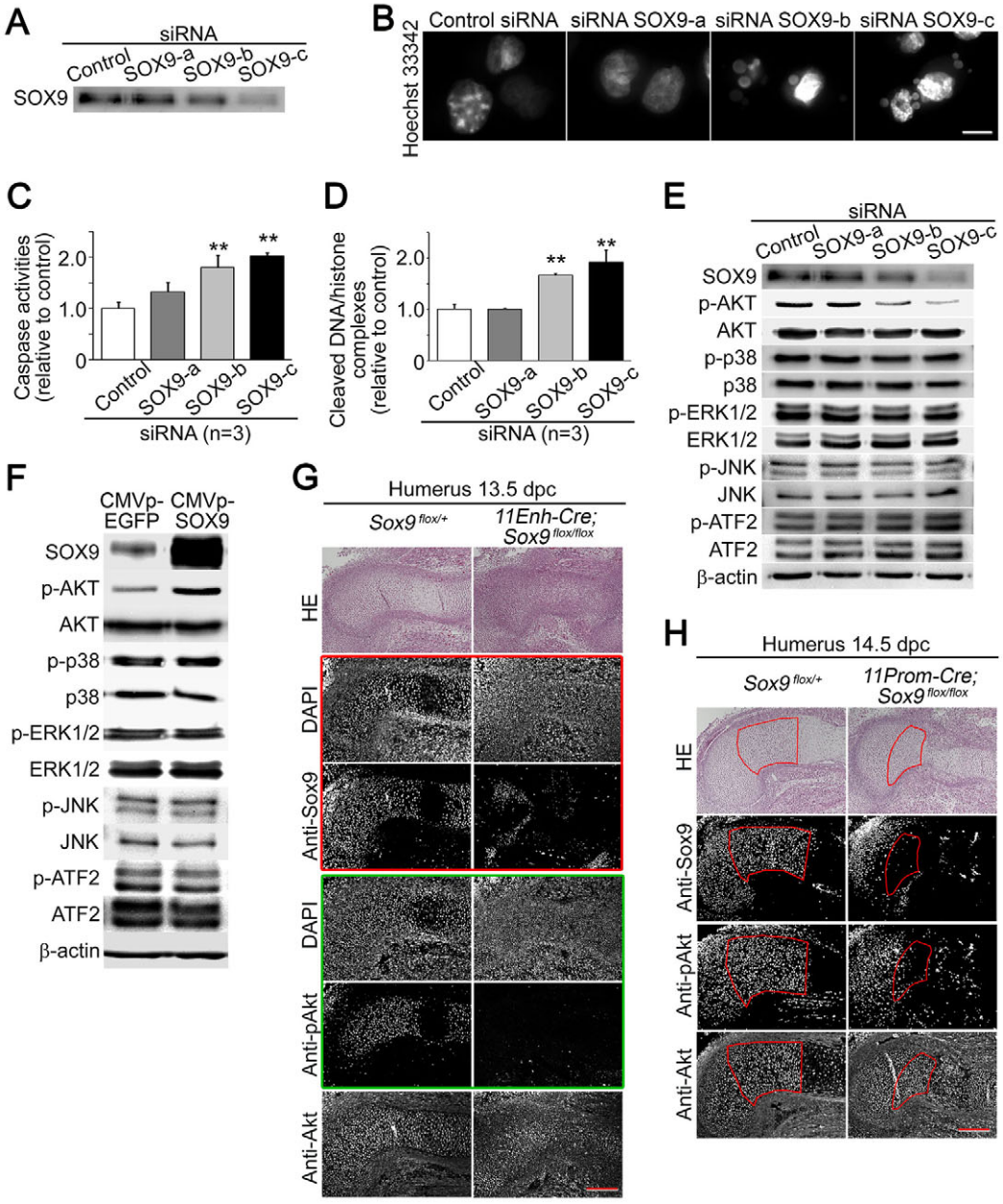

Fig. 4. Apoptosis of SW1353 chondrosarcoma cells by SOX9 knockdown and Akt phosphorylation in SW1353 cells and mice. (**A**) Immunoblot analysis of SOX9 expression in human SW1353 chondrosarcoma cells transfected with either of three different sets of SOX9 siRNAs (Invitrogen). Control shows Stealth RNAi negative control (Invitrogen). (**B**) Hoechst-stained SW1353 cells transfected with each siRNA. (**C**) Transfection with siRNA SOX9-b or siRNA SOX9-c increased caspase 3/7 activities in SW1353 cells. (**D**) Transfection with siRNA SOX9-b or siRNA SOX9-c increased the amount of cleaved DNA-histone complexes in SW1353 cells. Data (C,D) are mean + s.d. **, $P<0.01$. (**E**) Immunoblot analysis of SW1353 cells transfected with SOX9 siRNAs. (**F**) Immunoblot analysis of SW1353 cells transfected with either CMV promoter-EGFP (control) or CMV promoter-SOX9 (SOX9 overexpression). (**G**) Semi-serial sections of *Sox9*$^{flox/+}$ and *11Enh-Cre; Sox9*$^{flox/flox}$ samples as shown in Fig. 1C stained with HE or DAPI or immunostained for Sox9, Akt or phosphorylated (p) Akt. Sections immunostained with anti-Sox9 and anti-pAkt were double stained with DAPI, showing that these two sections are comparable. (**H**) Semi-serial sections of *Sox9*$^{flox/+}$ and *11Prom-Cre; Sox9*$^{flox/flox}$ humerus at 14.5 dpc. Metaphyseal flat proliferative chondrocytes are outlined (red line) in *Sox9*$^{flox/+}$ humerus (left panels). Metaphyseal proliferative chondrocytes that did not express Sox9, indicating that their *Sox9* gene was deleted (*Sox9*$^{flodelx/floxdel}$ chondrocytes), are outlined in *11Prom-Cre; Sox9*$^{flox/flox}$ humerus (right panels). *Sox9*$^{flodelx/floxdel}$ proliferative chondrocytes showed decreased immunoreactivity to anti-pAkt as compared with flat proliferative chondrocytes in control *Sox9*$^{flox/+}$ mice. Scale bars: 10 μm in B; 200 μm in G,H.

SOX9 knockdown-induced apoptosis of SW1353 chondrosarcoma cells

Next, we examined whether Sox9 is important for the survival of chondrosarcoma cells in vitro. To knockdown *SOX9* mRNA, we transfected human SW1353 chondrosarcoma cells with small interfering RNA (siRNA) using the Amaxa nucleofection technique, which yields high transfection efficiencies (see Fig. S5A in the supplementary material), and harvested the cells 6 hours later. SW1353 cells transfected with SOX9-c siRNA showed a dramatic decrease in SOX9 protein, whereas SOX9-b siRNA yielded a moderate decrease and SOX9-a siRNA did not affect the level of SOX9 protein (Fig. 4A). Hoechst-stained SW1353 cells transfected with siRNA SOX9-b and siRNA SOX9-c exhibited typical apoptotic morphology characterized by chromatin condensation and DNA fragmentation (Fig. 4B). The decrease in SOX9 expression (Fig. 4A) correlated with the increase in caspase 3/7 activities (Fig. 4C) and the amount of cleaved DNA-histone complexes (nucleosomes) (Fig. 4D) in SW1353 cells. These results suggest that the cell survival mechanism that requires SOX9 is also active in SW1353 chondrosarcoma cells. A possible explanation for the rapid death of SW1353 cells is that these chondrosarcoma cells undergo rapid cell cycles, such that the outcome of loss of SOX9 is quickly realized. Transfection of human HeLa cells or osteoblastic Saos2 cells with SOX9 siRNAs did not cause apoptosis; this result is consistent with the lack of SOX9 expression in these cell types (see Fig. S5B-D in the supplementary material). Thus, Sox9 is specifically needed for the survival of chondrocyte lineage cells, including chondrocytes and chondrosarcoma cells.

Akt phosphorylation is involved in the chondrocyte apoptosis induced by *Sox9* deletion

We next investigated the molecular mechanism of Sox9-induced survival of chondrocyte lineage cells. We first examined the activation of signaling molecules in SW1353 chondrosarcoma cells by western blot analysis. SOX9 knockdown specifically decreased the phosphorylation level of AKT, but it did not affect the phosphorylation levels of p38 mitogen-activated protein kinase (p38 MAPK; MAPK14 – Human Genome Nomenclature Committee), extracellular signal-regulated kinase (ERK), Jun N-terminal kinase (JNK) and activating transcription factor 2 (ATF2) (Fig. 4E). Consistently, the overexpression of SOX9 specifically increased the phosphorylation level of AKT, but did not change the phosphorylation levels of other signaling molecules (Fig. 4F).

We then examined phosphorylation in vivo. Immunohistochemical analysis showed that phospho-Akt was below detectable levels in both the control *Sox9*$^{flox/+}$ and *11Enh-Cre; Sox9*$^{flox/flox}$ mice at 12.5 dpc (Fig. S5E in the supplementary material). Phospho-Akt was detected in the central part of primordial cartilage and not in the periphery, whereas Sox9 was detected both in the central and peripheral parts of primordial cartilage in the control *Sox9*$^{flox/+}$ mice at 13.5 dpc (Fig. 4G). The area of *Sox9* deletion was limited to the central part of cartilage in *11Enh-Cre; Sox9*$^{flox/flox}$ mice and appeared to cover the area of phospho-Akt in the control *Sox9*$^{flox/+}$ mice at 13.5 dpc. Phospho-Akt was not detected in *11Enh-Cre; Sox9*$^{flox/flox}$ cartilage at 13.5 dpc (Fig. 4G), nor in *Sox9*$^{floxdel/floxdel}$ proliferative chondrocytes in *11Prom-Cre; Sox9*$^{flox/flox}$ mice (Fig. 4H). There were no obvious differences in the levels of phosphorylated Atf2, Jnk or p38 Mapk, as detected by antibody, between *Sox9*$^{floxdel/floxdel}$ proliferative chondrocytes in *11Prom-Cre; Sox9*$^{flox/flox}$ mice and proliferating chondrocytes in *Sox9*$^{flox/+}$ mice (see Fig. S5F in the supplementary material).

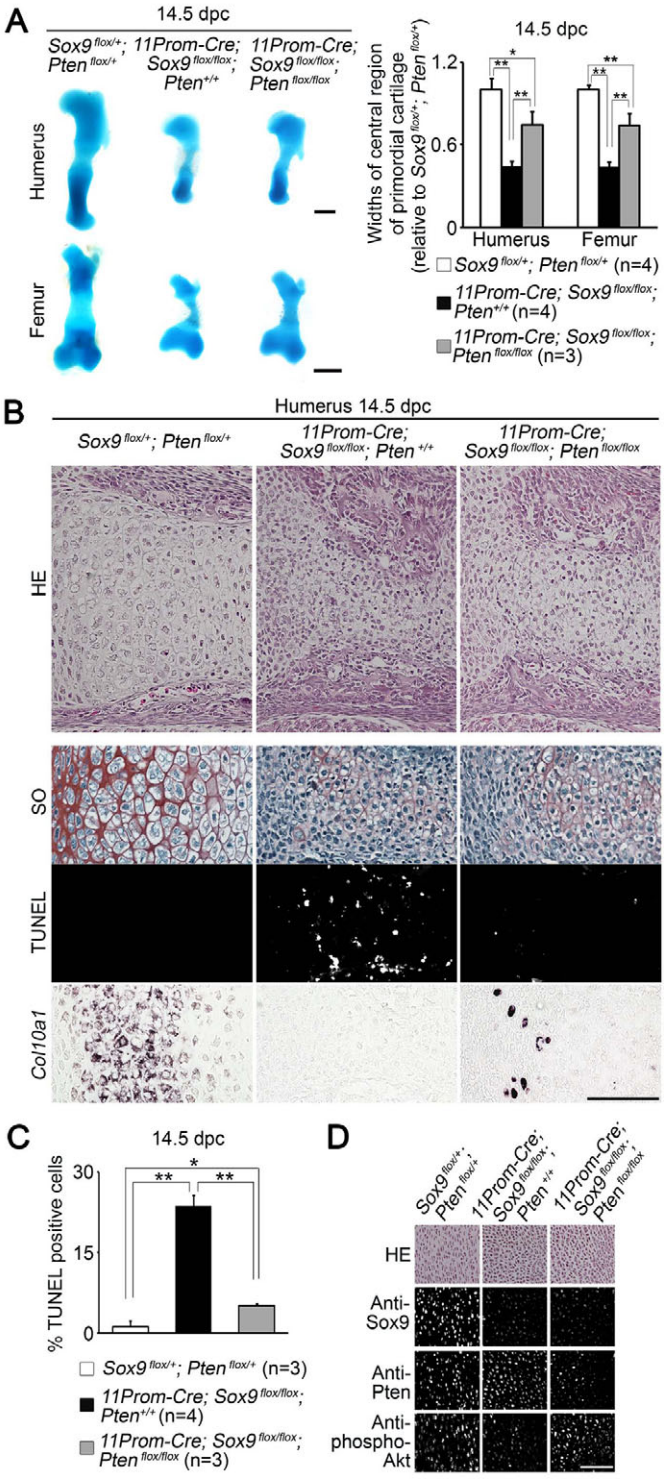

Fig. 5. Inactivation of *Pten* partially rescues the survival of *Sox9*$^{floxdel/floxdel}$ chondrocytes and *Col10a1* expression. (**A**) Humeral and femoral cartilaginous mouse skeletons at 14.5 dpc stained with Alcian Blue. (**B**) Central regions of the humerus at 14.5 dpc stained with HE or SO, hybridized with *Col10a1* cRNA probe or subjected to the TUNEL assay, as labeled. (**C**) The percentage of TUNEL-positive cells among the total cell number. (**D**) Sox9, Pten and pAkt immunohistochemistry of proliferative chondrocytes in the metaphyseal regions of the humerus from mice of the indicated genotypes. Data (A,C) are mean + s.d. *, $P<0.05$; **, $P<0.01$. Scale bars: 200 μm in A; 100 μm in B,D.

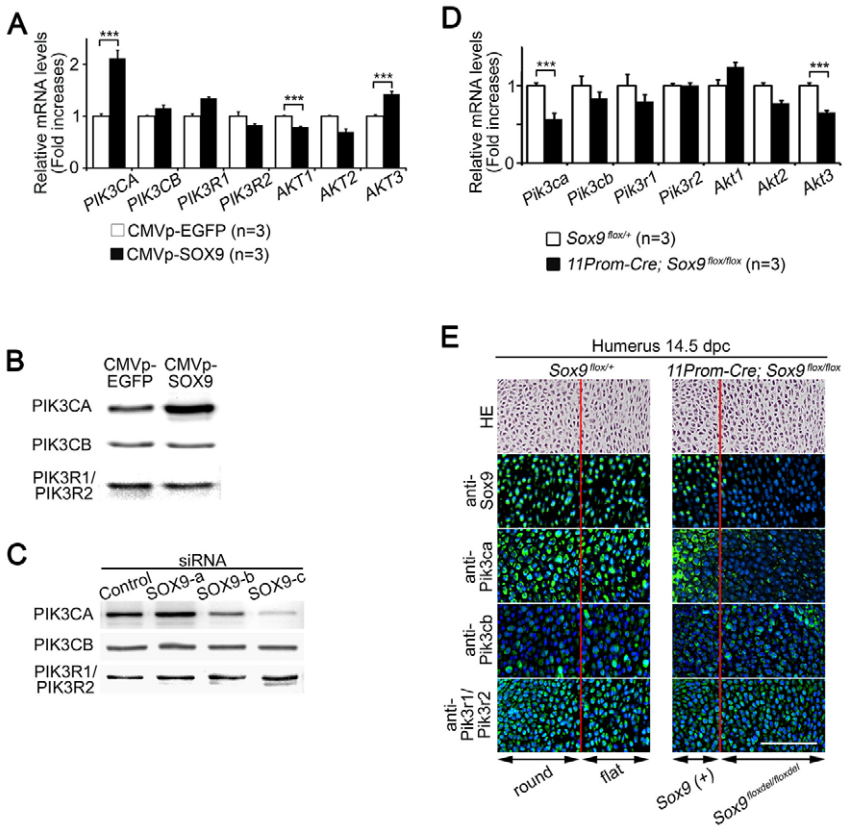

Fig. 6. Regulation of expression of *PIK3CA* by Sox9. (**A**) Real-time RT-PCR analysis of PIK3 and AKT gene expression in human SW1353 cells transfected with CMV promoter-EGFP (control) or CMV promoter-SOX9 (SOX9 overexpression). The expression levels of the genes in cells transfected with CMV promoter-EGFP were set at 1. (**B**) Immunoblot analysis of SW1353 cells transfected with CMV promoter-EGFP (control) or CMV promoter-SOX9 (SOX9 overexpression). (**C**) Immunoblot analysis of SW1353 cells transfected with SOX9 siRNA. Degrees of SOX9 knockdown by each siRNA are shown in Fig. 4A. (**D**) Real-time RT-PCR analysis of humerus from *Sox9*$^{flox/+}$ and *11Prom-Cre; Sox9*$^{flox/flox}$ mice. The expression levels of the genes in *Sox9*$^{flox/+}$ humerus were set at 1. Data (A,D) are mean + s.d. ***, P<0.0001. (**E**) HE staining and immunohistochemistry for the indicated proteins (green) counterstained with DAPI (blue) in proximal humeral cartilage at 14.5 dpc. (Left) For cartilage of *Sox9*$^{flox/+}$ mice, the red line indicates the transition between the round and flat proliferative chondrocyte zones. Sox9, Pik3ca, Pik3cb and Pik3r1/Pik3r2 were expressed both in round and flat proliferative chondrocytes. (Right) In cartilage of *11Prom-Cre; Sox9*$^{flox/flox}$ mice, anti-Sox9 revealed a boundary (red line) between chondrocytes in which the *Sox9* gene was not deleted and was expressed [*Sox9* (+)] and chondrocytes in which the *Sox9* gene was deleted and was not expressed (*Sox9*$^{floxdel/floxdel}$). Immunoreactivity against anti-Pik3ca decreased in *Sox9*$^{floxdel/floxdel}$ chondrocytes. Scale bar: 50 μm.

We next examined whether reduced phosphorylation of Akt is responsible for *Sox9* deletion-mediated chondrocyte apoptosis. We prepared *11Prom-Cre; Sox9*$^{flox/flox}$; *Pten*$^{flox/flox}$ double conditional knockout mice. Pten (phosphatase and tensin homolog) is a lipid phosphatase, the major substrate of which is PtdIns(3,4,5)P_3. Thus, the deletion of *Pten* results in the accumulation of PtdIns(3,4,5)P_3, leading to forced activation of Akt. *Col2a1-Cre; Pten*$^{flox/flox}$ mice show increased phosphorylation of Akt (Ford-Hutchinson et al., 2007; Yang et al., 2008). At 14.5 dpc, Alcian Blue staining of the skeleton showed that the degree of deformity of humeral cartilage in *11Prom-Cre; Sox9*$^{flox/flox}$; *Pten*$^{flox/flox}$ mice was milder than that in *11Prom-Cre; Sox9*$^{flox/flox}$; *Pten*$^{+/+}$ mice (Fig. 5A). The constriction of central regions of the humerus was also significantly milder. Histological analysis showed that the decreased cell numbers in the center of the cartilage, the excess number of TUNEL-positive cells and the loss of *Col10a1* expression in *11Prom-Cre; Sox9*$^{flox/flox}$; *Pten*$^{+/+}$ mice were partly restored in *11Prom-Cre; Sox9*$^{flox/flox}$; *Pten*$^{flox/flox}$ mice (Fig. 5B,C). Pten expression was decreased in *Sox9*$^{floxdel/floxdel}$; *Pten*$^{floxdel/floxdel}$ proliferative chondrocytes in *11Prom-Cre; Sox9*$^{flox/flox}$; *Pten*$^{flox/flox}$ mice (Fig. 5D and see Fig. S6 in the supplementary material). Phosphorylation levels of Akt in *Sox9*$^{floxdel/floxdel}$; *Pten*$^{floxdel/floxdel}$ proliferative chondrocytes were higher than those of *Sox9*$^{floxdel/floxdel}$; *Pten*$^{+/+}$ proliferative chondrocytes. Thus, both *Sox9* deletion and elevated Akt phosphorylation occurred in flat chondrocyte regions and the resulting modulation of apoptosis became apparent subsequently, when cells differentiated into terminally mature chondrocytes. These results suggest that decreased *Col10a1* expression and increased apoptosis induced by *Sox9* deletion are partly restored by the additional deletion of *Pten*, which restores Akt phosphorylation.

Regulation of expression of Pik3ca by Sox9

We used expression analysis and the candidate approach to investigate the molecular mechanism underlying the regulation of Akt phosphorylation by Sox9. We found that the expression of Pik3ca was regulated by Sox9. Pik3ca (also known as p110α) is one of three subunit proteins of phosphatidylinositol 3-kinase (PI3K). PI3K generates phosphatidylinositol (3,4,5)-trisphosphate [PtdIns(3,4,5)P_3] from PtdIns(4,5)P_2. PtdIns(3,4,5)P_3 causes phosphorylation of and activates Akt (Brazil et al., 2004). PI3K-Akt signaling regulates cell death (Cantley, 2002).

The regulation of PIK3CA expression by SOX9 was detected in SW1353 chondrosarcoma cells in vitro. Among genes encoding PI3K subunits, *PIK3CA* mRNA was induced by SOX9 overexpression (Fig. 6A). The expression levels of genes encoding the other PI3K subunits and AKT members were little affected by SOX9 overexpression. *PIK3CG* and *PIK3CD* (also known as *p110*γ and *p110*δ, respectively) mRNAs were not detected in SW1353 cells. Western blot analysis of SW1353 cell lysates showed that SOX9 overexpression increased PIK3CA protein levels but did not affect PIK3CB (p110β) or PIK3R1 (p85α)/PIK3R2 (p85β) protein levels (Fig. 6B). Consistently, SOX9 knockdown decreased PIK3CA protein levels but did not affect PIK3CB or PIK3R1/PIK3R2 protein levels (Fig. 6C).

The Sox9-mediated regulation of *Pik3ca* expression was also detected in vivo. Real-time RT-PCR analysis confirmed that *Pik3ca* expression was significantly decreased in *11Prom-Cre; Sox9*$^{flox/flox}$ humeral cartilage as compared with the expression level in control *Sox9*$^{flox/+}$ cartilage (Fig. 6D). Immunohistochemical analysis showed that Pik3ca immunoreactivity decreased in proliferative chondrocytes that did not express Sox9 (*Sox9*$^{floxdel/floxdel}$) as

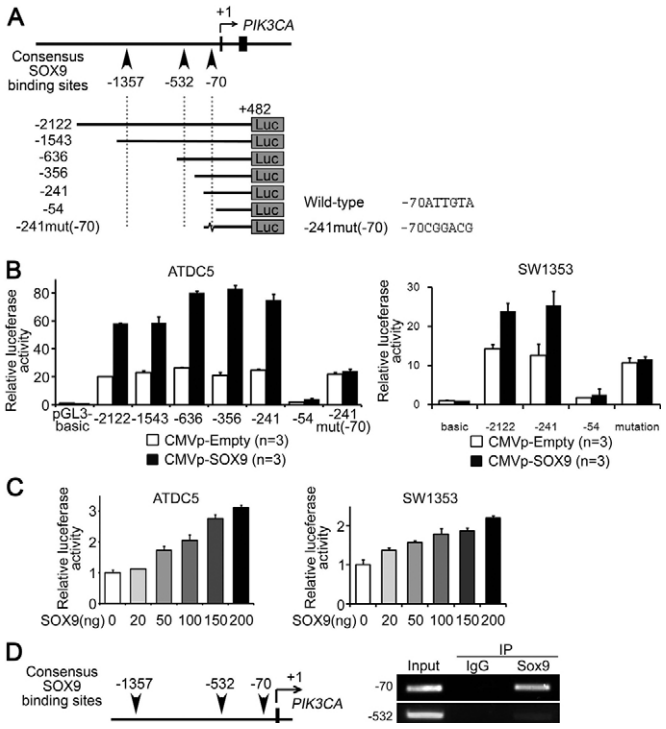

Fig. 7. Promoter analysis of *PIK3CA*. (**A**) Schematic representation of the human *PIK3CA* promoter region. Consensus SOX9 binding sites are indicated by arrowheads. Numbers indicate the distance (bp) from the transcription start site (+1, arrow). Beneath are shown the reporter gene constructs that contain various lengths of the promoter (upstream extent indicated to the left), followed by the Photinus luciferase gene (Luc). The substitution mutations (sequence changes illustrated to right) were introduced at the consensus SOX9 binding site at –70 in the –241 reporter to generate the –241mut(–70) reporter gene. (**B**) Reporter gene assays in undifferentiated mouse ATDC5 cells (top) and human SW1353 cells (bottom) with various *PIK3CA* reporter gene constructs. The mean luciferase activity of cells transfected with pGL3-basic vector without SOX9 was set at 1. (**C**) SOX9 enhanced the activity of the –2122 reporter gene in a dose-dependent manner in undifferentiated ATDC5 cells and SW1353 cells. The mean luciferase activity of cells without SOX9 transfection was set at 1. Data (B,C) are mean + s.d. (**D**) Chromatin immunoprecipitation analysis showed that SOX9 binds at around –70 bp in the *PIK3CA* promoter in SW1353 cells. IP, immunoprecipitation with IgG (negative control) or anti-Sox9 antibodies.

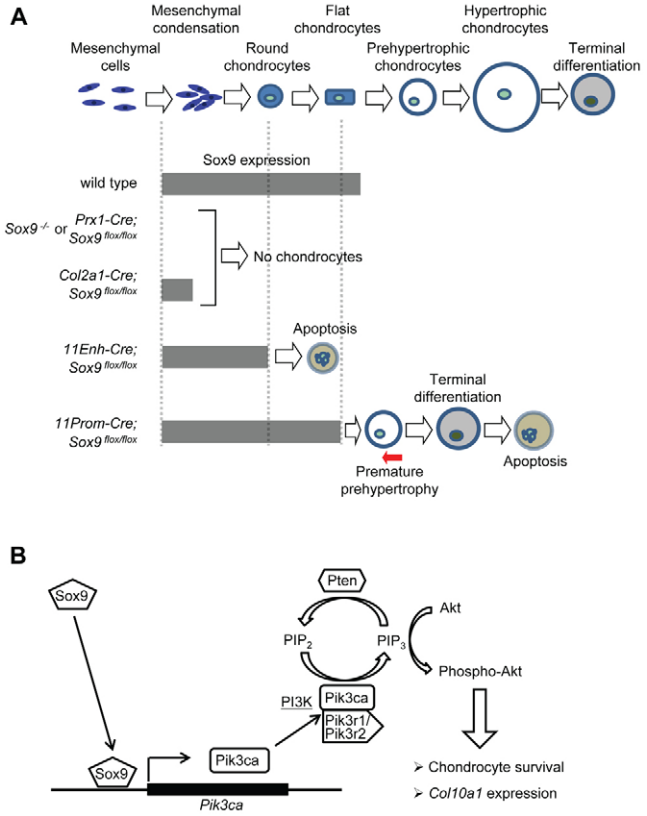

Fig. 8. Functions of Sox9 during chondrocyte differentiation. (**A**) The consequences of *Sox9* deletion at various steps during the chondrocyte differentiation process. (**B**) Summary of Sox9 functions in chondrocytes.

compared with Sox9-expressing chondrocytes in *11Prom-Cre; Sox9$^{flox/flox}$* mice (Fig. 6E), whereas the immunoreactivities of Pik3cb and Pik3r1/Pik3r2 were not obviously changed (Fig. 6E).

SOX9 binds and upregulates the *PIK3CA* promoter

We examined the possibility that SOX9 directly controls *PIK3CA* transcription. DNA sequence analysis of human *PIK3CA* revealed several putative SOX9 binding sites around the transcription start site that are conserved in the mouse and rat *Pik3ca* genes (Fig. 7A). Co-transfection of either undifferentiated mouse ATDC5 or human SW1353 cells with SOX9 stimulated the promoter activities of luciferase reporter constructs bearing 241 bp or longer *PIK3CA* promoters (Fig. 7B). SOX9 enhanced the activity of the 2122 bp promoter in a dose-dependent manner (Fig. 7C), whereas the 54 bp reporter constructs showed weak promoter activities regardless of the presence or absence of SOX9 (Fig. 7B). One consensus SOX9 binding site exists between –241 bp and –54 bp, at –70 bp (Fig. 7A). The stimulating effect of SOX9 on the 241 bp promoter was strongly impaired when a mutation was introduced into this consensus SOX9 binding site (Fig. 7B).

Evidence of SOX9 binding to the *PIK3CA* promoter in vivo was provided by chromatin immunoprecipitation (ChIP) of fragmented DNA from SW1353 chondrosarcoma cells using a primer pair that is specific for the –70 bp consensus SOX9 binding region (Fig. 7D). SOX9 binding was not detected when primer pairs specific for the other consensus sites were used. These results suggest that SOX9 binds to the *PIK3CA* promoter region to enhance its activities.

DISCUSSION

In the present study, immunohistochemical analysis with anti-Sox9 antibodies clearly demonstrated *Sox9* deletion patterns in conditional knockout mice. Fig. 8A shows a schematic representation of stages when *Sox9* genes are inactivated during the chondrocyte differentiation process in *Sox9* conditional knockout mice bearing each *Cre* transgene.

In *Col2a1-Cre; Sox9$^{flox/flox}$* conditional knockout mice, most chondroprogenitor cells are arrested as condensed mesenchymal cells, whereas a few cells differentiate into chondrocytes and undergo hypertrophy (Akiyama et al., 2002), suggesting the co-existence of a small population of chondroprogenitor cells in which Cre-mediated deletion does not occur and thus the chondrocyte differentiation program runs. By contrast, there were no

hypertrophic chondrocytes in *11Enh-Cre; Sox9*$^{flox/flox}$ and *11Prom-Cre; Sox9*$^{flox/flox}$ mice, suggesting that *Sox9* genes were inactivated uniformly at specific stages of chondrocyte differentiation.

Along with cellular differentiation processes, chondrocytes are believed to undergo apoptosis after going through hypertrophy. Our results show that Sox9 inactivation in round chondrocytes caused premature apoptosis and that Sox9 inactivation in flat chondrocytes caused immediate terminal maturation without hypertrophy and with excessive apoptosis (Fig. 8A). SOX9 knockdown caused apoptosis of SW1353 chondrosarcoma cells. Sox9 is expressed in progenitor cells in various organs (Akiyama et al., 2005), whereas most differentiated cell types, including osteoblasts and adipocytes, do not express Sox9 and survive. These findings suggest that chondrocytes survive by a mechanism that is sustained by Sox9. An association between Sox9 and cell survival has been shown in other cell lineages and tumors. Sox9 is transiently expressed in premigratory neural crest cells during development, and the loss of Sox9 results in apoptosis of neural crest cells (Cheung et al., 2005). Sox9 sustains the survival of neurofibromatosis tumor cell lines (Miller et al., 2009). Sox9 is expressed in the prostate epithelia and promotes prostate tumor cell proliferation and cooperates with Pten loss to drive tumor formation (Thomsen et al., 2010). However, the mechanisms by which Sox9 promotes cell survival were unknown. Our results suggest that Sox9 directly binds to the promoter region of the PI3K subunit gene *Pik3ca*, enhancing the phosphorylation of Akt. It will be of interest to investigate the roles of Sox5 and Sox6 in the regulation of PI3K subunit expression, e.g. to analyze *Pik3ca* expression in chondrocytes of *Sox5*$^{-/-}$; *Sox6*$^{-/-}$ mice. Forced phosphorylation of Akt by *Pten* inactivation partially restored cell survival of *Sox9*$^{floxdel/floxdel}$ chondrocytes. Thus, the chondrocyte-specific anti-apoptotic mechanism includes PI3K-Akt pathways that are activated by Sox9 (Fig. 8B). Because the restoration was partial, other as yet unknown mechanisms also contribute to the Sox9-dependent survival of chondrocytes. Our results showing that SOX9 regulates *PIK3CA* transcription suggest that cell death occurs cell-autonomously in SW1353 cells, although we speculate that non-cell-autonomous pathways also contribute to chondrocyte death. Decreased *Col2a1* expression in *Sox9*$^{floxdel/floxdel}$ chondrocytes results in reduced extracellular matrix, which might cause non-cell-autonomous chondrocyte death, especially in vivo. It is also possible that increased apoptosis in the terminal mature chondrocytes of *11Prom-Cre* mice might reflect an acceleration of the whole process of terminal maturation, including their removal via apoptosis. Because Sox9 does not appear to increase phospho-Akt levels in the prostate (Thomsen et al., 2010), the mechanisms by which Sox9 sustains cell survival might differ between tissues.

The PI3K-Akt pathway in chondrocytes has been studied extensively. *Akt* knockout mice show delayed calcification (Chen et al., 2001; Fukai et al., 2010; Peng et al., 2003), whereas calcification is increased in *11Prom-Cre; Sox9*$^{flox/flox}$ mice. Osteoblasts in *11Prom-Cre; Sox9*$^{flox/flox}$ mice are not affected. A possible explanation for this discrepancy is that delayed ossification in *Akt* knockout mice is caused by *Akt* deletion in osteoblasts or bone collar cells. Akt signaling enhances chondrocyte proliferation (Kita et al., 2008) and PI3K decreases apoptosis (Ulici et al., 2008), consistent with the phenotypes of *11Prom-Cre; Sox9*$^{flox/flox}$ mice. The effects on hypertrophy are controversial, as PI3K enhances hypertrophy (Fujita et al., 2004), whereas Akt signaling inhibits hypertrophy (Kita et al., 2008). The phenotypes of *11Prom-Cre; Sox9*$^{flox/flox}$ mice appear to be consistent with the former. Discrepancies might reflect the complex downstream pathways of Akt, as Akt regulates chondrocyte proliferation and differentiation through GSK3, mTOR and FoxOs differently (Rokutanda et al., 2009). Taken together with the finding that Akt-GSK3 pathways are relatively unimportant in vertebral bodies (Rokutanda et al., 2009), the very small primordial cartilage of the vertebral bodies and limbs in *11Prom-Cre; Sox9*$^{flox/flox}$ mice suggests that Akt-mTOR and Akt-FoxO pathways mediate the chondrocyte survival mechanism that is sustained by Sox9.

Previous in vivo and in vitro studies have implied that Sox9 inhibits the hypertrophy of chondrocytes, thus maintaining proliferating chondrocyte characteristics (Akiyama et al., 2004; Bi et al., 2001). By contrast, our results show that *Sox9* deletion in flat chondrocytes results in an absence of hypertrophic chondrocytes and in immediate terminal differentiation. Sox9 interacts with Runx2 and represses its activities (Zhou et al., 2006). Our results revealed that the Runx2 expression level is increased in Sox9-deficient chondrocytes, indicating that Sox9 also directly or indirectly inhibits *Runx2* at the level of transcription. The expression of *Col1a1*, but not *Col10a1*, was activated in Sox9-deficient chondrocytes, although both genes are direct targets of Runx2 (Ducy et al., 1997; Zheng et al., 2003). This observation suggests that flat chondrocytes lacking Sox9 lose other components necessary for subsequent *Col10a1* expression and hypertrophy. It is also possible that decreased levels of phospho-Akt secondarily affect *Col10a1* expression. It is interesting that, in 13.5 dpc humerus, the premature shutdown of Sox9 expression by only a few cell layers causes dramatic changes in subsequent chondrocyte differentiation and survival. This suggests that expression of Sox9 to the very last stage of flat chondrocytes, just prior to hypertrophy, is essential for chondrocyte hypertrophy and for proper subsequent endochondral bone formation.

11Enh-Cre; Sox9$^{flox/+}$ embryos exhibited a straight radius and ulna (see Fig. S1E,F in the supplementary material). By contrast, campomelic dysplasia, which is associated with mutations in a single allele of *SOX9*, is characterized by the bending of long bones (Foster et al., 1994; Wagner et al., 1994). Bowing and angulation of the radius and ulna are also seen in *Sox9*$^{+/-}$ mouse embryos (Bi et al., 2001). These results suggest that skeletal bending is caused by Sox9 deficiency at the mesenchymal cell stage.

In summary, our results from *11Enh-Cre; Sox9*$^{flox/flox}$ and *11Prom-Cre; Sox9*$^{flox/flox}$ mice and from SOX9 knockdown in human chondrosarcoma cells suggest that the expression of Sox9 in differentiated chondrocyte lineage cells is essential for cell survival. Sox9 in differentiated chondrocytes is also needed for subsequent hypertrophy and proper endochondral bone formation in mice. Sox9 sustains cell survival at least partly through its binding to the *Pik3ca* promoter, inducing Akt phosphorylation. Understanding Sox9 function in differentiated chondrocytes will contribute both to maintaining cartilage homeostasis and treating chondrosarcoma.

Acknowledgements
We thank Junko Murai, Kunihiko Hiramatsu, Mari Shinkawa, Kanako Nakagawa, Mina Okamoto, Hidetatsu Outani and Satoru Sasagawa for assistance and helpful discussions; and Andreas Schedl for the preparation of *Sox9*$^{flox/flox}$ mice. This study was supported in part by Scientific Research Grants 18390415, 19659378 and 21390421 from MEXT and JST, CREST.

Competing interests statement
The authors declare no competing financial interests.

Supplementary material
Supplementary material for this article is available at
http://dev.biologists.org/lookup/suppl/doi:10.1242/dev.057802/-/DC1

References

Akiyama, H., Chaboissier, M. C., Martin, J. F., Schedl, A. and de Crombrugghe, B. (2002). The transcription factor Sox9 has essential roles in successive steps of the chondrocyte differentiation pathway and is required for expression of Sox5 and Sox6. *Genes Dev.* **16**, 2813-2828.

Akiyama, H., Lyons, J. P., Mori-Akiyama, Y., Yang, X., Zhang, R., Zhang, Z., Deng, J. M., Taketo, M. M., Nakamura, T., Behringer, R. R. et al. (2004). Interactions between Sox9 and beta-catenin control chondrocyte differentiation. *Genes Dev.* **18**, 1072-1087.

Akiyama, H., Kim, J. E., Nakashima, K., Balmes, G., Iwai, N., Deng, J. M., Zhang, Z., Martin, J. F., Behringer, R. R., Nakamura, T. et al. (2005). Osteo-chondroprogenitor cells are derived from Sox9 expressing precursors. *Proc. Natl. Acad. Sci. USA* **102**, 14665-14670.

Bi, W., Deng, J. M., Zhang, Z., Behringer, R. R. and de Crombrugghe, B. (1999). Sox9 is required for cartilage formation. *Nat. Genet.* **22**, 85-89.

Bi, W., Huang, W., Whitworth, D. J., Deng, J. M., Zhang, Z., Behringer, R. R. and de Crombrugghe, B. (2001). Haploinsufficiency of Sox9 results in defective cartilage primordia and premature skeletal mineralization. *Proc. Natl. Acad. Sci. USA* **98**, 6698-6703.

Brazil, D. P., Yang, Z. Z. and Hemmings, B. A. (2004). Advances in protein kinase B signalling: AKTion on multiple fronts. *Trends Biochem. Sci.* **29**, 233-242.

Brew, C. J., Clegg, P. D., Boot-Handford, R. P., Andrew, J. G. and Hardingham, T. (2010). Gene expression in human chondrocytes in late osteoarthritis is changed in both fibrillated and intact cartilage without evidence of generalised chondrocyte hypertrophy. *Ann. Rheum. Dis.* **69**, 234-240.

Cantley, L. C. (2002). The phosphoinositide 3-kinase pathway. *Science* **296**, 1655-1657.

Chen, W. S., Xu, P. Z., Gottlob, K., Chen, M. L., Sokol, K., Shiyanova, T., Roninson, I., Weng, W., Suzuki, R., Tobe, K. et al. (2001). Growth retardation and increased apoptosis in mice with homozygous disruption of the Akt1 gene. *Genes Dev.* **15**, 2203-2208.

Cheung, M., Chaboissier, M. C., Mynett, A., Hirst, E., Schedl, A. and Briscoe, J. (2005). The transcriptional control of trunk neural crest induction, survival, and delamination. *Dev. Cell* **8**, 179-192.

Ducy, P., Zhang, R., Geoffroy, V., Ridall, A. L. and Karsenty, G. (1997). Osf2/Cbfa1: a transcriptional activator of osteoblast differentiation. *Cell* **89**, 747-754.

Ford-Hutchinson, A. F., Ali, Z., Lines, S. E., Hallgrimsson, B., Boyd, S. K. and Jirik, F. R. (2007). Inactivation of Pten in osteo-chondroprogenitor cells leads to epiphyseal growth plate abnormalities and skeletal overgrowth. *J. Bone Miner. Res.* **22**, 1245-1259.

Foster, J. W., Dominguez-Steglich, M. A., Guioli, S., Kwok, C., Weller, P. A., Stevanovic, M., Weissenbach, J., Mansour, S., Young, I. D., Goodfellow, P. N. et al. (1994). Campomelic dysplasia and autosomal sex reversal caused by mutations in an SRY-related gene. *Nature* **372**, 525-530.

Fujita, T., Azuma, Y., Fukuyama, R., Hattori, Y., Yoshida, C., Koida, M., Ogita, K. and Komori, T. (2004). Runx2 induces osteoblast and chondrocyte differentiation and enhances their migration by coupling with PI3K-Akt signaling. *J. Cell Biol.* **166**, 85-95.

Fukai, A., Kawamura, N., Saito, T., Oshima, Y., Ikeda, T., Kugimiya, F., Higashikawa, A., Yano, F., Ogata, N., Nakamura, K. et al. (2010). Akt1 in murine chondrocytes controls cartilage calcification during endochondral ossification under physiologic and pathologic conditions. *Arthritis Rheum.* **62**, 826-836.

Hattori, T., Muller, C., Gebhard, S., Bauer, E., Pausch, F., Schlund, B., Bosl, M. R., Hess, A., Surmann-Schmitt, C., von der Mark, H. et al. (2010). SOX9 is a major negative regulator of cartilage vascularization, bone marrow formation and endochondral ossification. *Development* **137**, 901-911.

Hui, R. C., Gomes, A. R., Constantinidou, D., Costa, J. R., Karadedou, C. T., Fernandez de Mattos, S., Wymann, M. P., Brosens, J. J., Schulze, A. and Lam, E. W. (2008). The forkhead transcription factor FOXO3a increases phosphoinositide-3 kinase/Akt activity in drug-resistant leukemic cells through induction of PIK3CA expression. *Mol. Cell. Biol.* **28**, 5886-5898.

Iwai, T., Murai, J., Yoshikawa, H. and Tsumaki, N. (2008). Smad7 Inhibits chondrocyte differentiation at multiple steps during endochondral bone formation and down-regulates p38 MAPK pathways. *J. Biol. Chem.* **283**, 27154-27164.

Kita, K., Kimura, T., Nakamura, N., Yoshikawa, H. and Nakano, T. (2008). PI3K/Akt signaling as a key regulatory pathway for chondrocyte terminal differentiation. *Genes Cells* **13**, 839-850.

Lefebvre, V. and Smits, P. (2005). Transcriptional control of chondrocyte fate and differentiation. *Birth Defects Res. C Embryo Today* **75**, 200-212.

Miller, S. J., Jessen, W. J., Mehta, T., Hardiman, A., Sites, E., Kaiser, S., Jegga, A. G., Li, H., Upadhyaya, M., Giovannini, M. et al. (2009). Integrative genomic analyses of neurofibromatosis tumours identify SOX9 as a biomarker and survival gene. *EMBO Mol. Med.* **1**, 236-248.

Ng, L. J., Wheatley, S., Muscat, G. E., Conway-Campbell, J., Bowles, J., Wright, E., Bell, D. M., Tam, P. P., Cheah, K. S. and Koopman, P. (1997). SOX9 binds DNA, activates transcription, and coexpresses with type II collagen during chondrogenesis in the mouse. *Dev. Biol.* **183**, 108-121.

Pelton, R. W., Dickinson, M. E., Moses, H. L. and Hogan, B. L. (1990). In situ hybridization analysis of TGF beta 3 RNA expression during mouse development: comparative studies with TGF beta 1 and beta 2. *Development* **110**, 609-620.

Peng, X. D., Xu, P. Z., Chen, M. L., Hahn-Windgassen, A., Skeen, J., Jacobs, J., Sundararajan, D., Chen, W. S., Crawford, S. E., Coleman, K. G. et al. (2003). Dwarfism, impaired skin development, skeletal muscle atrophy, delayed bone development, and impeded adipogenesis in mice lacking Akt1 and Akt2. *Genes Dev.* **17**, 1352-1365.

Peters, P. W. J. (1977). Double staining of fetal skeletons for cartilage and bone. In *Methods in Prenatal Toxicology* (ed. H. J. M. D. Neuberg and T. E. Kwasigroch), pp. 153-154. Stuttgart, Germany: Georg Thieme Verlag.

Rokutanda, S., Fujita, T., Kanatani, N., Yoshida, C. A., Komori, H., Liu, W., Mizuno, A. and Komori, T. (2009). Akt regulates skeletal development through GSK3, mTOR, and FoxOs. *Dev. Biol.* **328**, 78-93.

Sakai, K. and Miyazaki, J. (1997). A transgenic mouse line that retains Cre recombinase activity in mature oocytes irrespective of the cre transgene transmission. *Biochem. Biophys. Res. Commun.* **237**, 318-324.

Shukunami, C., Shigeno, C., Atsumi, T., Ishizeki, K., Suzuki, F. and Hiraki, Y. (1996). Chondrogenic differentiation of clonal mouse embryonic cell line ATDC5 in vitro: differentiation-dependent gene expression of parathyroid hormone (PTH)/PTH-related peptide receptor. *J. Cell Biol.* **133**, 457-468.

Smits, P., Li, P., Mandel, J., Zhang, Z., Deng, J. M., Behringer, R. R., de Crombrugghe, B. and Lefebvre, V. (2001). The transcription factors L-Sox5 and Sox6 are essential for cartilage formation. *Dev. Cell* **1**, 277-290.

Smits, P., Dy, P., Mitra, S. and Lefebvre, V. (2004). Sox5 and Sox6 are needed to develop and maintain source, columnar, and hypertrophic chondrocytes in the cartilage growth plate. *J. Cell Biol.* **164**, 747-758.

Suzuki, A., Yamaguchi, M. T., Ohteki, T., Sasaki, T., Kaisho, T., Kimura, Y., Yoshida, R., Wakeham, A., Higuchi, T., Fukumoto, M. et al. (2001). T cell-specific loss of Pten leads to defects in central and peripheral tolerance. *Immunity* **14**, 523-534.

Thomsen, M. K., Ambroisine, L., Wynn, S., Cheah, K. S., Foster, C. S., Fisher, G., Berney, D. M., Moller, H., Reuter, V. E., Scardino, P. et al. (2010). SOX9 elevation in the prostate promotes proliferation and cooperates with PTEN loss to drive tumor formation. *Cancer Res.* **70**, 979-987.

Ulici, V., Hoenselaar, K. D., Gillespie, J. R. and Beier, F. (2008). The PI3K pathway regulates endochondral bone growth through control of hypertrophic chondrocyte differentiation. *BMC Dev. Biol.* **8**, 40.

Wagner, T., Wirth, J., Meyer, J., Zabel, B., Held, M., Zimmer, J., Pasantes, J., Bricarelli, F. D., Keutel, J., Hustert, E. et al. (1994). Autosomal sex reversal and campomelic dysplasia are caused by mutations in and around the SRY-related gene SOX9. *Cell* **79**, 1111-1120.

Wang, Y. and Sul, H. S. (2009). Pref-1 regulates mesenchymal cell commitment and differentiation through Sox9. *Cell Metab.* **9**, 287-302.

Yang, G., Sun, Q., Teng, Y., Li, F., Weng, T. and Yang, X. (2008). PTEN deficiency causes dyschondroplasia in mice by enhanced hypoxia-inducible factor 1alpha signaling and endoplasmic reticulum stress. *Development* **135**, 3587-3597.

Zhao, Q., Eberspaecher, H., Lefebvre, V. and De Crombrugghe, B. (1997). Parallel expression of Sox9 and Col2a1 in cells undergoing chondrogenesis. *Dev. Dyn.* **209**, 377-386.

Zheng, Q., Zhou, G., Morello, R., Chen, Y., Garcia-Rojas, X. and Lee, B. (2003). Type X collagen gene regulation by Runx2 contributes directly to its hypertrophic chondrocyte-specific expression in vivo. *J. Cell Biol.* **162**, 833-842.

Zhou, G., Zheng, Q., Engin, F., Munivez, E., Chen, Y., Sebald, E., Krakow, D. and Lee, B. (2006). Dominance of SOX9 function over RUNX2 during skeletogenesis. *Proc. Natl. Acad. Sci. USA* **103**, 19004-19009.

Table S1. Primers used in real-time RT-PCR

Primer	Sequence (5′ to 3′)
Col10a1 S	CCAATGCAGAATCAAACGG
Col10a1 AS	TGGAAAGCCTTTCTAAGCG
Pik3ca S	CCACGACCATCTTCGGGTG
Pik3ca AS	ACGGAGGCATTCTAAAGTCACTA
Pik3cb S	CTATGGCAGACAACCTTGACAT
Pik3cb AS	CTTCCCGAGGTACTTCCAACT
Pik3r1 S	ACACCACGGTTTGGACTATGG
Pik3r1 AS	GGCTACAGTAGTGGGCTTGG
Pik3r2 S	GGATGCCTGGCTTCAACGA
Pik3r2 AS	CTGGGAGTATGTGGCCTGACT
Akt1 S	ATGAACGACGTAGCCATTGTG
Akt1 AS	TTGTAGCCAATAAAGGTGCCAT
Akt2 S	ACGTGGTGAATACATCAAGACC
Akt2 AS	GCTACAGAGAAATTGTTCAGGGG
Akt3 S	TGGGTTCAGAAGAGGGGAGAA
Akt3 AS	AGGGGATAAGGTAAGTCCACATC
PIK3CA S	ACCAGTAGGCAACCGTGAAG
PIK3CA AS	TGGCGGATAGACATACATTGCT
PIK3CB S	CCTTTTGCCCACTGGGATTTA
PIK3CB AS	AGGTCTGACATCACAGAGTCTT
PIK3R1 S	AAAGGGTCCTTAGTAGCTCTTGG
PIK3R1 AS	CGTAAGTTCCCGGAAAGTCCC
PIK3R2 S	GTCCGAGATGCTTCTAGCAAG
PIK3R2 AS	CAGCTTATTGTTCCCGCCTTT
AKT1 S	GCACAAACGAGGGGAGTACAT
AKT1 AS	CCTCACGTTGGTCCACATC
AKT2 S	CAAGCGTGGTGAATACATCAAGA
AKT2 AS	GCCTCTCCTTGTACCCAATGA
AKT3 S	AAGGTTGGGTTCAGAAGAGGG
AKT3 AS	TGAGGGGATAAGGTAAATCCACA

Table S2. siRNAs

siRNA	Invitrogen Cat. No.	Target sequence (5′ to 3′)
SOX9-a	SOX9-HSS186044	CAGCACUGGGAACAACCCGUCUACA
SOX9-b	SOX9-HSS110099	UGAAGAAGGAGAGCGAGGAGGACAA
SOX9-c	SOX9-HSS110100	GCAAGCUCUGGAGACUUCUGAACGA

Table S3. Primers used in ChIP assay

Primer	Sequence (5′ to 3′)
–70 S	CCCAACTGTACATAAACTTCGG
–70 AS	CTCCGGCAGAAGAGGGTAAGA
–532 S	GTCTCCACGAAGTGAGTCAAA
–532 AS	CACCCATAGAGGAAACGAGATTA
–1357 S	GTGGATCACCTGAAGTCAGAA
–1357 AS	CCAGAGTCTCACTCTGTAGC